

---

# GRADIENTSPACE: UNSUPERVISED DATA CLUSTERING FOR IMPROVED INSTRUCTION TUNING

---

Shrihari Sridharan<sup>1</sup> Deepak Ravikumar<sup>1</sup> Anand Raghunathan<sup>1</sup> Kaushik Roy<sup>1</sup>

## ABSTRACT

Instruction tuning is one of the key steps required for adapting large language models (LLMs) to a broad spectrum of downstream applications. However, this procedure is difficult because real-world datasets are rarely homogeneous; they consist of a mixture of diverse information, causing gradient interference, where conflicting gradients pull the model in opposing directions, degrading performance. A common strategy to mitigate this issue is to group data based on semantic or embedding similarity. However, this fails to capture how data influences model parameters during learning. While recent works have attempted to cluster gradients directly, they randomly project gradients into lower dimensions to manage memory, which leads to accuracy loss. Moreover, these methods rely on expert ensembles which necessitates multiple inference passes and expensive on-the-fly gradient computations during inference. To address these limitations, we propose GRADIENTSPACE, a framework that clusters samples directly in full-dimensional gradient space. We introduce an online SVD-based algorithm that operates on LoRA gradients to identify latent skills without the infeasible cost of storing all sample gradients. Each cluster is used to train a specialized LoRA expert along with a lightweight router trained to select the best expert during inference. We show that routing to a single, appropriate expert outperforms expert ensembles used in prior work, while significantly reducing inference latency. Our experiments across mathematical reasoning, code generation, finance, and creative writing tasks demonstrate that GRADIENTSPACE leads to coherent expert specialization and consistent accuracy gains over state-of-the-art clustering methods and finetuning techniques.

## 1 INTRODUCTION

Large language models (LLMs) like GPT (OpenAI et al., 2024), Llama (Grattafiori et al., 2024), and DeepSeek (DeepSeek-AI et al., 2025) have become integral components in modern AI systems such as conversational agents and chatbots due to their ability to generate coherent text that closely mirrors natural human communication. One of the key reasons for this success is instruction tuning, a procedure where pretrained models are finetuned on datasets that consist of human-written instructions paired with responses (Zhang et al., 2025c; Han et al., 2025).

Although instruction tuning has shown good efficacy, the datasets are usually curated from a single source or belong to a specific domain, which limits their ability to generalize across diverse real-world data distributions (Ghosh et al., 2024; Han et al., 2025). For example, when building an internal knowledge assistant within an organization, the underlying training data may include a mixture of documents, emails, support tickets, and wiki pages. Re-

cent works (Bukharin et al., 2024; Chen et al., 2024; Wu et al., 2024a) have demonstrated that when instructions are mixed naively from different datasets, the performance of the model degrades. This is primarily due to a phenomenon called gradient interference (Yu et al., 2020; Shi et al., 2023), where examples corresponding to distinct tasks or domains push model parameters in conflicting directions. Learning from diverse sources is challenging because the model must reconcile competing learning signals, leading to negative transfer and reduced overall performance.

To address this challenge, previous efforts have explored strategies to mitigate gradient interference. One such approach groups training examples by semantic similarity, assuming that semantically related inputs would influence compatible parameter updates (Rao et al., 2024; Ge et al., 2024). However, input similarity is not a reliable proxy for how the model learns these inputs. Two semantically similar inputs may produce opposing gradients, while unrelated examples can reinforce each other if their updates are aligned. As shown in Figure 4, gradient and semantic similarities show little correlation, highlighting the need for organizing data based on learning dynamics. A different line of research, known as gradient surgery, modifies gradients during training to remove conflicts. Methods such as (Yu

<sup>1</sup>School of Electrical and Computer Engineering, Purdue University. Correspondence to: Shrihari Sridharan <sridhar4@purdue.edu>.

et al., 2020) and (Liu et al., 2024) project gradients from different tasks onto non-conflicting subspaces to reduce interference. However, these approaches rely on explicit task labels to project gradients, which limits their applicability to real-world instruction tuning.

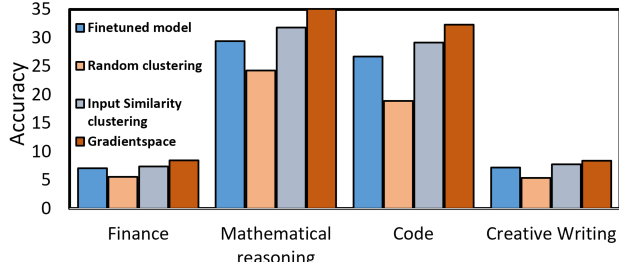


Figure 1. GRADIENTSPACE accuracy compared to other methods on different benchmarks.

This motivates a fundamental question: “*How should finetuning data be partitioned effectively when task boundaries are unknown?*” To address this, we introduce GRADIENTSPACE, a framework that clusters data based on gradient similarity and groups samples that produce positively correlated parameter updates. GRADIENTSPACE naturally identifies latent “skills” within unlabeled data by clustering examples that produce positively aligned gradient updates. Theoretically, this is equivalent to the covariance term in the gradient variance decomposition, showing that grouping examples with high positive covariance reduces gradient interference and improves Stochastic Gradient Descent (SGD) convergence (more details in Section 4). Recent work from (Li et al., 2025) takes a similar approach, building ensembles with LoRA adaptors on gradient-clustered data. However, such an approach requires computing and storing gradients for every input sample, which is infeasible; consequently, they down-project the gradients into a lower dimension, losing performance. This is a general issue for calculating sample influence, such as in LESS (Xia et al., 2024).

To address this, we develop a novel online learning methodology which handles LoRA gradients in full dimensionality, thus making full use of the gradient signals. This is performed by first training a LoRA adapter (Hu et al., 2022) on a warm-up dataset to obtain meaningful gradient representations and adapt the model to the input data distribution. Next, online singular value decomposition (SVD)-based clustering is performed, where SVD over the gradient matrix is employed to estimate the number of latent clusters and initialize their centroids based on the dominant gradient directions. This ensures that clustering begins in a subspace capturing the most significant gradient variance. Centroids are then refined using an exponential moving

average (EMA) update. Next, each discovered cluster is finetuned into a specialized LoRA expert.

While identifying clusters and training a LoRA expert for each is essential, a fast inference method is also needed. Techniques such as (Li et al., 2025) employ gradient similarity during inference to identify the right set of experts; this can be very expensive, unrealistic for production deployment, and result in suboptimal accuracy. Our solution to this comes from two novel contributions: (a) we show that a correctly chosen cluster with a single expert adaptor is in fact better than an ensemble (4.2% on average better than Li et al. (2025)), and (b) we introduce a fast, lightweight router trained on the resulting cluster assignments to dynamically select the most appropriate expert during inference, reducing computational cost compared to (Li et al., 2025), as shown in Table 4. The three-stage pipeline of the proposed GRADIENTSPACE method is illustrated in Figure 2.

We evaluate GRADIENTSPACE across multiple domains including mathematical reasoning, code generation, finance, and creative writing across several benchmarks. Our results, as shown in Figure 1, produces coherent expert specialization and improved task accuracy, outperforming both state-of-the-art clustering baselines and other finetuning methods.

## 2 BACKGROUND

In this section, we explain preliminaries and notations we use in the rest of our paper.

**Notation.** In this subsection we describe the notation used in this paper. For our setup consider the next token prediction problem. That is let  $x_i \sim X$  represent a sequence of tokens, and  $y_i \sim Y|X$  be the corresponding next token for the sequence  $x_i$ . Then the goal is to learn a function  $g : x_i \mapsto y_i$  using a neural net  $f_\theta$  parametrized by  $\theta$ . This is done by optimizing the loss function  $\mathcal{L}$  over the dataset  $\mathcal{D} = \{(x_1, y_1), (x_2, y_2), \dots, (x_N, y_N)\}$ .

**$\rho$ -Lipschitz Gradient.** The loss function  $\mathcal{L}$  is said to be  $\rho$ -smooth (i.e., its gradient  $\nabla \mathcal{L}$  is  $\rho$ -Lipschitz) on the domain  $\text{Range}(\theta)$  if there exists a constant  $\rho > 0$  such that for all  $\theta_1, \theta_2 \in \text{Range}(\theta)$ :

$$\|\nabla \mathcal{L}(\theta_1) - \nabla \mathcal{L}(\theta_2)\| \leq \rho \|\theta_1 - \theta_2\| \quad (1)$$

**Bounded Gradient Variance.** Often for SGD convergence assumption under non convex settings (Ghadimi & Lan, 2013) assume the expected squared  $\ell_2$ -norm of the stochastic gradients is uniformly bounded by a constant  $\sigma^2$ .

**Stochastic Gradient Descent (SGD).** We briefly recall the SGD update and a nonconvex convergence result following Ghadimi & Lan (2013). Let  $f(\theta)$  denote the (possibly nonconvex) objective and let  $g_t$  be a stochastic gradient satis-

fying  $\mathbb{E}[g_t | \theta_t] = \nabla \mathcal{L}(\theta_t)$  and  $\mathbb{E}[\|g_t - \nabla \mathcal{L}(\theta_t)\|^2 | \theta_t] \leq \sigma^2$ . The SGD update is

$$\theta_{t+1} = \theta_t - \eta_t g_t. \quad (2)$$

Under  $\rho$ -Lipschitz gradients and a decreasing stepsize, e.g.  $\eta_t = \min\left\{\frac{1}{\rho}, \frac{\tilde{D}}{\sigma\sqrt{T}}\right\}$  for  $t = 1, \dots, T$ , if we return a random iterate  $\theta_R$  uniformly from  $\{\theta_1, \dots, \theta_T\}$ , then

$$\frac{1}{\rho} \mathbb{E}[\|\nabla \mathcal{L}(\theta_R)\|^2] \leq \frac{\rho D_f^2}{T} + \frac{2D_f\sigma}{\sqrt{T}}, \quad (3)$$

where  $D_f = \sqrt{\frac{2(\mathcal{L}(\theta_1) - \mathcal{L}^*)}{\rho}}$ . Hence, the expected gradient norm decreases at rate  $O(1/\sqrt{T})$  in the nonconvex setting.

### 3 RELATED WORK

In this section, we categorize prior work into four categories: Training Dynamics and Gradient Alignment, Gradient-based data selection, Dataset Partitioning, Mixture of LoRA experts and compare GRADIENTSPACE with each of them.

**Training Dynamics and Gradient Alignment.** Gradient interference occurs when different training examples induce conflicting updates, reducing learning efficiency in multi-task or heterogeneous datasets. (Yu et al., 2020) and (Liu et al., 2024), project gradients to mitigate conflicts, while (Shi et al., 2023) creates task-specific branches for high-conflict layers. However, these methods require explicit task labels to identify and resolve conflicts. To that end, token-level techniques such as (Yang et al., 2025) analyze intra-expert gradient conflicts without task labels but rely on specialized routing and architecture. GRADIENTSPACE takes a data-centric approach where we partition the dataset so each expert receives gradient-aligned examples requiring no task labels. Moreover, (Yang et al., 2025) is complementary to GRADIENTSPACE and can be applied alongside our method for improved performance.

**Gradient-based Data Selection.** There have been various data selection methods proposed to identify high quality subsets from large heterogeneous datasets. (Wang et al., 2025) employs gradient-based clustering to select training samples, using cosine similarities of gradients computed with respect to pretrained models to identify influential data points. Similarly, (Zhang et al., 2025b) introduces task-agnostic gradient clustered coresset selection, applying K-means clustering on gradient features to gather samples with similar characteristics for efficient instruction tuning. Other gradient-based selection approaches (Xia et al., 2024; Kwon et al., 2024; Nagaraj et al., 2025) include influence function methods (Koh & Liang, 2017) that prioritize samples based on Hessians and loss trajectories. While these methods demonstrate usage of gradient information for identifying important training samples, they fundamentally differ from

our approach in that they select subsets of data rather than partition the entire dataset for training.

**Gradient-based clustering.** ELREA (Li et al., 2025) proposed clustering data based on gradients to train expert adapters and combine them with weighted averaging. During inference, they compute the gradient of the input and route to an ensemble of experts. However, there are two issues. First, ELREA relies on random projections to lower gradient dimension which causes information loss. Second, their approach requires computing gradients during inference which is computationally expensive for each input and multiple inference passes since they utilize expert ensembles. In contrast, GRADIENTSPACE clusters samples based on gradients using an online SVD-based clustering method utilizing full gradient dimension. This ensures that each expert learns from gradient aligned examples, allowing us to route to a single optimal expert during inference. We also design a lightweight router to determine the most optimal expert to route to during inference, leading to negligible latency overhead.

**Dataset Partitioning.** Several works have explored partitioning instruction datasets into coherent groups for improved training efficiency. (Rao et al., 2024) introduces commonality-aware instruction tuning, partitioning datasets using three distinct metrics: task clustering based on task labels, embedding clustering using semantic embeddings, and length clustering based on response characteristics. Beyond topical or length cues, (Ge et al., 2024) first filters high-quality pairs, then applies embedding-based clustering to form diverse partitions for tuning. These semantic-based partitioning approaches focus on surface-level similarities between instructions, such as topic coherence or syntactic patterns. However, they do not consider the optimization dynamics and interference that arise during gradient-based training.

**Mixture of LoRA experts.** Mixture of LoRA Experts (Wu et al., 2024b) and its variants (Schafhalter et al., 2024), (Zhang et al., 2025a), (Li et al., 2024), and (Mu et al., 2025) extends parameter efficient finetuning by combining multiple LoRA adapters through learned gating and routing to enable task specialization within a single model. These methods include features such as hierarchical gating, adaptive rank selection, and load balanced expert routing to merge or activate adapters efficiently. In contrast, GRADIENTSPACE adopts a data-centric approach; instead of defining how experts are combined, we determine what data should each expert be trained on by clustering samples in gradient space. This ensures that each expert learns from gradient-aligned examples without relying on predefined task boundaries.

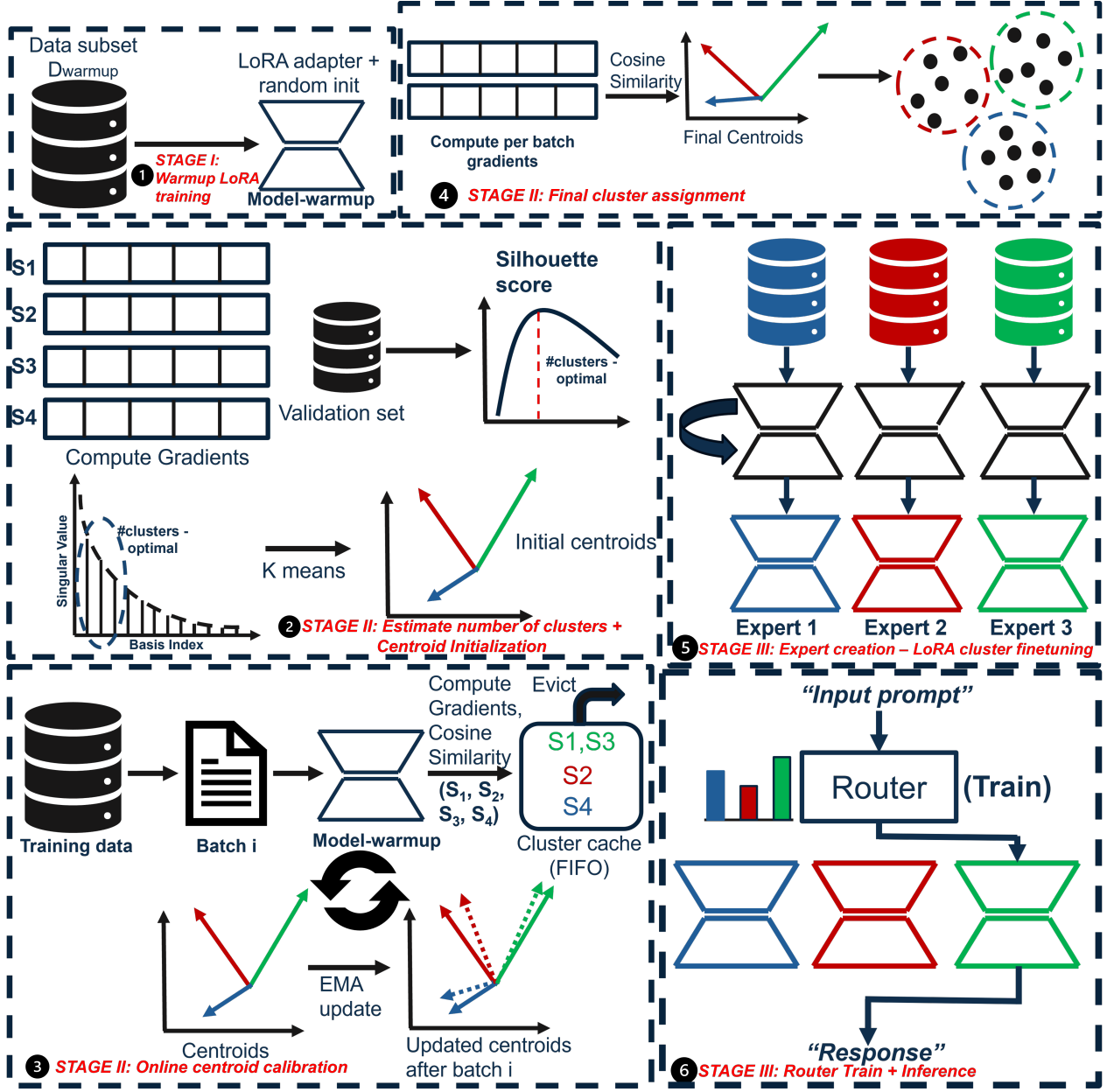


Figure 2. GRADIENTSPACE framework. Stage I (LoRA warm-up): train a small LoRA adapter on a warm-up split to obtain meaningful, low-dimensional gradient representations. Stage II (online SVD clustering): estimate  $K$  via SVD on a validation gradient matrix, initialize centroids in the dominant gradient subspace, then refine them online with a cluster cache and EMA updates to form gradient-aligned partitions. Stage III (experts + router): finetune one LoRA expert per cluster and use a lightweight encoder-based router to select the most appropriate expert at inference.

## 4 THEORETICAL FORMULATION

In this section, we present a formal analysis supporting the claims of the GRADIENTSPACE framework. Before we present our results we define a few terms. Let  $\mathcal{D}$  be a dataset, and let  $\{\mathcal{D}_1, \mathcal{D}_2, \dots, \mathcal{D}_k\}$  be a partition of  $\mathcal{D}$  (i.e.,  $\bigcup_{i=1}^k \mathcal{D}_i = \mathcal{D}$  and  $\mathcal{D}_i \cap \mathcal{D}_j = \emptyset$  for  $i \neq j$ ). Let

$\{\nabla \mathcal{L}_i(\theta)\}_{i=1}^k$  be the gradient vectors for these subsets.

**Lemma 1** Let  $\alpha_1, \dots, \alpha_k \in [0, 1]$  such that  $\sum_{i=1}^k \alpha_i = 1$ . Define the combined gradient  $\nabla \mathcal{L}(\theta)$  as:

$$\nabla \mathcal{L}(\theta) := \sum_{i=1}^k \alpha_i \nabla \mathcal{L}_i(\theta).$$

Then the variance of the combined gradient is given by:

$$\begin{aligned} \text{Var}(\nabla \mathcal{L}(\theta)) &= \sum_{i=1}^k \alpha_i^2 \text{Var}(\nabla \mathcal{L}_i(\theta)) \\ &+ \sum_{i \neq j} \alpha_i \alpha_j \text{Cov}(\nabla \mathcal{L}_i(\theta), \nabla \mathcal{L}_j(\theta)) \end{aligned} \quad (4)$$

**Sketch of Proof.** At a high level, the result follows from the standard variance decomposition rule. The combined gradient is a weighted sum of the gradients from each subset, so its total variance naturally splits into two parts: the weighted sum of the individual (within-subset) variances and the cross-term capturing how gradients from different subsets co-vary. This yields the stated expression for the variance of the combined gradient. The proof is provided in the Appendix.

**Interpreting Theory.** The lemma shows that training on a mixture of subsets aggregates two noise sources: the intrinsic gradient variance within each subset and the cross-subset covariance. In the GRADIENTSPACE setting, routing to coherent subsets reduces within-subset dispersion and suppresses harmful cross-covariances, recovering the “experts converge faster” intuition: per-subset (expert) updates omit the cross terms, yielding lower gradient variance and tighter expected  $\varepsilon$ -stationarity guarantees than a shared model that mixes conflicting gradients.

Next, we establish a result showing that training on subsets identified by GRADIENTSPACE yields a reduction in gradient variance.

**Theorem 2 (Variance Reduction)** *Let  $\text{Var}(d)$  denote the variance of the gradients computed on a dataset  $d$ . Let a dataset  $\mathcal{D}$  be partitioned into subsets  $\{\mathcal{D}_1, \mathcal{D}_2, \dots, \mathcal{D}_k\}$  using the GRADIENTSPACE method. Then for any subset  $\mathcal{D}_i$  in the partition:*

$$\text{Var}(\mathcal{D}_i) \leq \text{Var}(\mathcal{D}) \quad \text{for all } i \in \{1, \dots, k\}. \quad (5)$$

**Sketch of Proof.** The result follows from the law of total variance. When the dataset  $\mathcal{D}$  is partitioned into subsets  $\{\mathcal{D}_i\}$  using the GRADIENTSPACE method, the total gradient variance decomposes into within-subset and between-subset components. The algorithm explicitly minimizes within-subset dispersion in gradient space, ensuring that each  $\mathcal{D}_i$  has gradients that are more homogeneous than the global set. Consequently, the within-subset variance  $\text{Var}(\mathcal{D}_i)$  cannot exceed the overall variance  $\text{Var}(\mathcal{D})$ , and is strictly smaller whenever subsets differ in their mean gradient directions. The proof is provided in the Appendix.

**Interpreting Theory.** This result shows that partitioning data in gradient space effectively separates examples with

conflicting gradient directions, thereby reducing gradient noise during optimization. Lower gradient variance leads to more stable updates and faster convergence under stochastic gradient descent. In this way, training on subsets identified by GRADIENTSPACE mirrors the advantage of expert models over shared models, each subset behaves as a low-variance expert, accelerating overall training dynamics.

Finally, we present the analysis on improved  $\varepsilon$ -stationarity when using GRADIENTSPACE.

**Definition (Expected  $\varepsilon$ -Stationarity).** An SGD training run is said to be *expected  $\varepsilon$ -stationary* after  $T$  steps if

$$\frac{1}{T} \sum_{t=0}^{T-1} \mathbb{E}[\|\nabla \mathcal{L}(\theta_t)\|^2] \leq \varepsilon,$$

that is, the average expected squared gradient norm across its iterates is at most  $\varepsilon$ . This indicates that, on average, the run has reached an  $\varepsilon$ -approximate stationary point of the loss surface. This definition is a modification of the standard  $\varepsilon$ -stationarity notion, where only the final iterate satisfies  $\|\nabla \mathcal{L}(\theta_T)\|^2 \leq \varepsilon$ . The updated definition simplifies formal analysis of non-convex SGD training.

We define the variance of the stochastic gradients for the full dataset and for each cluster  $i$  as:

$$\sigma_{\mathcal{D}}^2 = \text{Var}(\nabla \mathcal{L}_{\mathcal{D}}(\theta)), \quad \sigma_{\mathcal{D}_i}^2 = \text{Var}(\nabla \mathcal{L}_{\mathcal{D}_i}(\theta)).$$

From Theorem 2 we have  $\bar{\sigma}_{\text{cluster}}^2 \leq \sigma_{\mathcal{D}}^2$ . Let SGD <sub>$\mathcal{D}$</sub>  and SGD<sub>cluster</sub> be defined as above. Assume both algorithms (i) start from the same initialization  $\theta_0$ , (ii) use the same stepsize  $\eta \leq 1/\rho$ , (iii) and are run for the same number of iterations  $T$  on an  $\rho$ -smooth objective  $\mathcal{L}$  with unbiased gradient estimates. We group these three under the *SGD convergence assumptions*. Let  $\mathcal{L}^* := \inf_{\theta} \mathcal{L}(\theta)$ . Then their expected  $\varepsilon$ -stationarity levels after  $T$  steps satisfy

$$\varepsilon_{\mathcal{D}} \leq \frac{\eta\rho}{2T} (\mathcal{L}(\theta_0) - \mathcal{L}^*) + \rho\eta\sigma_{\mathcal{D}}^2, \quad (6)$$

$$\varepsilon_{\text{cluster}} \leq \frac{\eta\rho}{2T} (\mathcal{L}(\theta_0) - \mathcal{L}^*) + \rho\eta\bar{\sigma}_{\text{cluster}}^2. \quad (7)$$

As  $T \rightarrow \infty$ , the initial suboptimality gap term vanishes, making the asymptotic convergence behavior dominated by the variance terms. The ratio of these asymptotic bounds is

$$\lim_{T \rightarrow \infty} \frac{\varepsilon_{\text{cluster}}}{\varepsilon_{\mathcal{D}}} \leq \frac{\rho\eta\bar{\sigma}_{\text{cluster}}^2}{\rho\eta\sigma_{\mathcal{D}}^2} = \frac{\bar{\sigma}_{\text{cluster}}^2}{\sigma_{\mathcal{D}}^2}.$$

Since  $\bar{\sigma}_{\text{cluster}}^2 \leq \sigma_{\mathcal{D}}^2$ , this ratio is less than or equal to 1, demonstrating the asymptotic improvement in convergence to a stationary point. Hence we can write the following result.

**Theorem 3 (Asymptotic Stationarity Improvement)** *Under the SGD convergence assumptions, the ratio of the*

expected  $\varepsilon$ -stationarity bounds for  $\text{SGD}_{\text{cluster}}$  and  $\text{SGD}_{\mathcal{D}}$  satisfies

$$\lim_{T \rightarrow \infty} \frac{\varepsilon_{\text{cluster}}}{\varepsilon_{\mathcal{D}}} \leq \frac{\rho\eta\bar{\sigma}_{\text{cluster}}^2}{\rho\eta\sigma_{\mathcal{D}}^2} = \frac{\bar{\sigma}_{\text{cluster}}^2}{\sigma_{\mathcal{D}}^2}.$$

**Interpreting Theory.** Theorem 3 shows that in the asymptotic case, SGD driven by GRADIENTSPACE gradients is *provably closer to first-order stationarity* (i.e., has a smaller bound) than vanilla SGD on the full dataset. Equivalently, GRADIENTSPACE reaches an  $\varepsilon$ -stationary solution that is: it guarantees a lower expected gradient norm at the same training cost.

## 5 METHODOLOGY

We introduce GRADIENTSPACE, a framework that partitions heterogeneous instruction tuning data based on *gradient similarity* without any predefined task labels. GRADIENTSPACE operates in three stages. In **Stage I**, we train a LoRA adapter (Hu et al., 2022) using a small subset of data to adapt the model to the input data distribution. In **Stage II**, we group input samples with similar gradient updates using an online SVD-based clustering algorithm. Finally, in **Stage III**, we finetune the LoRA adapter from stage I for each discovered cluster to create experts and train a lightweight router to dynamically select the appropriate expert during inference. Figure 2 provides an overview of the proposed framework. We first explain the problem setup and describe each stage in detail below.

### 5.1 Problem Setup

Let  $\mathcal{D} = \{(x_i, y_i)\}_{i=1}^N$  be a finetuning dataset consisting of heterogeneous instruction samples. Given a model  $f_\theta$  with parameters  $\theta$ , the gradient of the loss  $\mathcal{L}$  for a sample  $(x_i, y_i)$  is

$$g_i = \nabla_\theta \mathcal{L}(f_\theta(x_i), y_i).$$

Two samples  $i, j$  are considered *gradient-aligned* if their cosine similarity

$$\text{sim}(g_i, g_j) = \frac{g_i^\top g_j}{\|g_i\| \|g_j\|}$$

is greater than a threshold. Intuitively, these samples push the model parameters in similar directions and can be optimized together without destructive interference. The objective of GRADIENTSPACE is to partition  $\mathcal{D}$  into  $K$  clusters  $\{\mathcal{D}_1, \mathcal{D}_2, \dots, \mathcal{D}_K\}$  that maximize intra-cluster gradient alignment while minimizing cross-cluster conflict. Formally, we define the objective as follows:

$$\begin{aligned} & \underset{\{D_k\}_{k=1}^K}{\text{maximize}} \quad \sum_{k=1}^K \sum_{i,j \in D_k} \text{sim}(g_i, g_j) \\ & \text{subject to} \quad \sum_{p \neq q} \sum_{i \in D_p, j \in D_q} \text{sim}(g_i, g_j) \text{ minimized.} \end{aligned} \quad (8)$$

### 5.2 Stage I: Gradient Approximation via LoRA Warm-up

We adopt the standard low rank adaptation (LoRA) method (Hu et al., 2022) to reduce the number of trainable parameters and enable more efficient gradient computations. LoRA achieves this by freezing the pretrained model weights and injecting trainable low-rank adapters into the linear layers distributed throughout the network. We use LoRA to instruction tune a pre-trained model (e.g., LLaMA-2-7B) on a small random subset  $\mathcal{D}_{\text{warmup}} \subset \mathcal{D}$  (5% of the training dataset) for a few epochs, training only the low-rank adapters  $\Delta\theta_{\text{LoRA}}$ . For each example  $(x_i, y_i) \in \mathcal{D}_{\text{warmup}}$ , we compute the gradient with respect to the LoRA parameters:

$$\tilde{g}_i = \nabla_{\Delta\theta_{\text{LoRA}}} L(f_{\theta, \Delta\theta_{\text{LoRA}}}(x_i), y_i),$$

which serves as a compact, low-dimensional representation of the full-parameter gradient. We primarily perform this step to obtain meaningful gradients in the next stages based on the input data distribution.

### 5.3 Stage II: Online SVD-based Clustering and Centroid Refinement

In this stage, we estimate the number of clusters for GRADIENTSPACE, initialize centroids using SVD and perform online gradient clustering to determine per sample alignment and refine the initialized centroids.

#### 5.3.1 Estimating number of clusters and centroid initialization

After the LoRA warm-up stage (Stage I), we now compute the gradient representations  $\{\tilde{g}_i\}_{i=1}^{n_{\text{val}}}$  for a small validation subset. These gradients capture the base model updates and serve as the input for identifying latent task structure. To organize the gradients into coherent groups, we represent each cluster by a *centroid*  $c_k \in \mathbb{R}^d$ , defined as the mean of all gradients assigned to that cluster. Each centroid thus represents the “average update direction” for a latent task, providing a compact summary of the gradients in that group and serving as a reference for clustering new examples.

To estimate the optimal number of clusters  $K$ , we perform singular value decomposition (SVD) on the gradient matrix  $G \in \mathbb{R}^{n_{\text{val}} \times d}$ , where each row corresponds to a gradient:

$$G = U \Sigma V^\top,$$

with  $\Sigma = \text{diag}(\sigma_1, \sigma_2, \dots, \sigma_r)$  containing the singular values. The explained variance ratio for the top- $k$  components is

$$\text{ExplainedVariance}(k) = \frac{\sum_{i=1}^k \sigma_i^2}{\sum_{i=1}^r \sigma_i^2},$$

quantifying the fraction of total gradient variance captured by the dominant directions.

For a range of variance thresholds (e.g., 80%–95%), we project the gradients onto the corresponding top- $k$  singular vectors:

$$\tilde{G}_k = GV_k,$$

where  $V_k \in \mathbb{R}^{d \times k}$  contains the top- $k$  right singular vectors. We then apply K-means clustering in this subspace, and the **Silhouette score** is computed to evaluate cluster coherence. The number of clusters  $K$  that yields the highest Silhouette score is selected as the optimal cluster count. We note that the highest silhouette score corresponds to the best accuracy as shown in section 6. Finally, the centroids  $\{c_k\}_{k=1}^K$  obtained from K-means in the SVD-projected space serve as the initial “prototype gradients” for each latent task, providing the starting points for subsequent online clustering across the full training dataset.

### 5.3.2 Online Centroid Calibration

After computing the initial centroids in the previous step, we perform online clustering to efficiently manage gradient assignments across the full dataset without storing all gradients simultaneously. For each incoming mini-batch of examples  $\mathcal{B}_t = \{(x_i, y_i)\}$ , we compute the corresponding set of low-dimensional gradients  $\tilde{G}_t = \{\tilde{g}_i\}_{i \in \mathcal{B}_t}$  and assign each gradient to the nearest centroid based on cosine similarity.

To maintain stable and adaptive clusters, we introduce a *cluster cache* that records recent gradient assignments for each centroid. This ensures the order of samples do not influence centroid creation disproportionately, which can occur if updates are computed solely from the current batch. By maintaining a rolling window of the most recent gradients assigned to each cluster, the centroids are re-evaluated using the average of the cached gradients. We implement the cluster cache as a fixed-size buffer for each cluster, discarding older entries in a first-in-first-out manner to ensure the centroids reflect recent and important gradient information.

The centroids themselves are updated incrementally using an exponential moving average (EMA). Formally, let  $C_k$  denote the fixed-size buffer (cluster cache) maintaining the most recent gradients assigned to cluster  $k$ :

$$c_k^{(t+1)} = \beta c_k^{(t)} + (1 - \beta) \frac{1}{|\mathcal{C}_k|} \sum_{g \in \mathcal{C}_k} \tilde{g},$$

where  $\beta \in [0, 1]$  controls the temporal smoothing. The

cluster cache size for each cluster  $k$  is set to  $|\mathcal{C}_k| = \alpha \cdot |\mathcal{B}_t|$ , where  $|\mathcal{B}_t|$  denotes the batch size and  $\alpha \in \mathbb{N}$  is a tunable scaling parameter. We find that values of  $\alpha$  in the range [5, 10] yield robust performance across diverse tasks, balancing stability and memory overhead. This refinement process is repeated for several epochs until the centroids converge, yielding the final set of stable centroids  $\{c_k^{(\text{final})}\}_{k=1}^K$ .

### 5.3.3 Final Cluster Assignment

After centroid refinement converges, we perform a final assignment pass over all samples to establish fixed cluster assignments. For each training example  $(x_i, y_i)$  with gradient representation  $\tilde{g}_i$ , we compute cosine similarity with all centroids and assign it to the most aligned one:

$$k_i = \arg \max_{k \in \{1, \dots, K\}} \text{sim}(\tilde{g}_i, c_k^{(\text{final})}), \quad (9)$$

where  $\text{sim}(\cdot, \cdot)$  denotes cosine similarity. This produces the final partition  $\{D_1, D_2, \dots, D_K\}$ , where each subset contains examples that induce mutually reinforcing gradient updates. The resulting assignments are subsequently used in Stage III to train cluster-specific LoRA experts and to supervise the router.

## 5.4 Stage III: Expert Specialization and Adaptive Routing

In this stage, we create experts by finetuning LoRA adapters (from Stage I) and train a router to select the optimal expert during inference.

### 5.4.1 Cluster-Specific Expert Fine-Tuning

After online clustering, each cluster  $\mathcal{D}_k$  forms the data foundation for a specialized LoRA expert. We instantiate  $K$  LoRA adapters  $\{\Delta\theta_{\text{LoRA}}^{(k)}\}_{k=1}^K$  and finetune each expert on its corresponding subset

$$\min_{\Delta\theta_{\text{LoRA}}^{(k)}} \frac{1}{|\mathcal{D}_k|} \sum_{(x_i, y_i) \in \mathcal{D}_k} \mathcal{L}(f_{\theta, \Delta\theta_{\text{LoRA}}^{(k)}}(x_i), y_i).$$

Each expert captures a distinct “skill” in the model’s parameter space, reflecting the structure of the discovered gradient clusters. Importantly, the base model remains frozen across all experts, thereby ensuring low training overhead. We note that we use the warmup up lora adapter rather than randomly initialized adapter since this helps in improving performance.

### 5.4.2 Router Training and Inference

We design a lightweight router that predicts the most appropriate expert for each input. As illustrated in Figure 3, the router is implemented as an encoder-based model in which

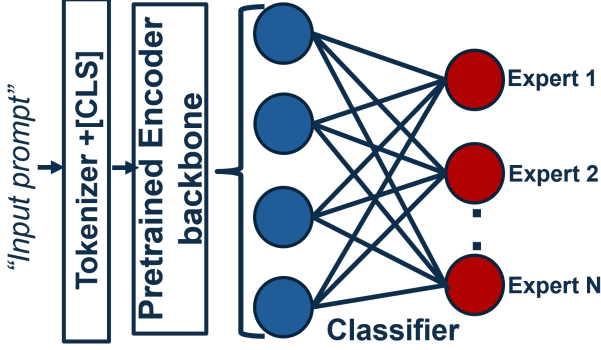


Figure 3. GRADIENTSPACE Router.

the standard classification head is replaced with a linear projection layer of dimension  $K$ , corresponding to the number of experts. During training, the encoder backbone is frozen, and only the final projection layer is updated.

Let  $h_i$  denote the fixed input representation extracted from the encoder (e.g., the final-layer hidden state or gradient-derived feature) corresponding to input  $x_i$ . The router takes  $h_i$  as input and outputs a distribution over clusters:

$$p_\phi(k | x_i) = \text{softmax}(W h_i + b),$$

where  $\phi = \{W, b\}$  are router parameters. It is trained using cross-entropy loss with the discovered cluster assignments as supervision:

$$\mathcal{L}_{\text{router}} = - \sum_i \log p_\phi(k_i | x_i).$$

During inference, the router assigns each input to the most relevant expert, and the final output is produced by that expert's LoRA adapter:

$$\hat{y} = f_{\theta, \Delta\theta_{\text{LoRA}}^{(k^*)}}(x), \quad k^* = \arg \max_k p_\phi(k | x).$$

We present the accuracy and latency results of this router compared to other state-of-the-art methods in section 6.4.

## 6 EXPERIMENTS

In this section we details the experiments to validate the claims of the paper.

### 6.1 Gradient vs Input Space

One of the motivations for this paper is that input similarity is not the same as learning similarity. In this section, we provide evidence for that claim. We test this hypothesis using the Llama 2-7B model and the mteb/stsbenchmark-sts dataset (Muennighoff et al., 2023). This dataset consists of

pairs of inputs with varying degrees of semantic similarity, where similarity between each pair is measured using cosine similarity between their embeddings. We show that high cosine similarity between a pair of inputs does not necessarily correspond to similar learning behavior.

**Experiment** We evaluate 500 human-annotated pairs and measure the gradients of the LoRA weights for Llama 2-7B and compute (i) cosine similarity between their input embeddings and (ii) cosine similarity between the corresponding LoRA gradients obtained from the model's parameter updates.

**Results and Takeaways** As shown in Figure 4, our results indicate that gradient similarity, which reflects how the model would update its parameters, is not predicted by input embedding similarity (shows poor correlation) confirming our previous hypothesis.

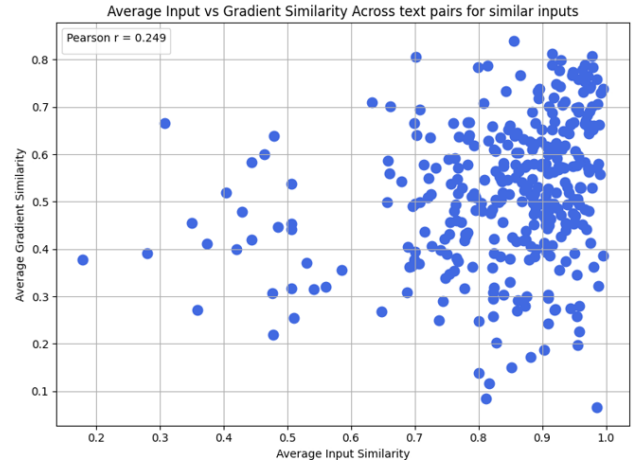


Figure 4. Comparison of input embedding similarity and gradient similarity across 500 randomly selected instruction pairs from the MTEB STS benchmark dataset using LLaMA-2-7B.

### 6.2 Instruction Tuning Experiments

We conduct experiments using two pretrained base models: LLaMA-2-7B (et al., 2023) and LLaMA-3.2-1B (Grattafiori et al., 2024). Both models are instruction-tuned under identical training configurations for fair comparison. For LoRA, we use  $r=32$  for all our experiments. We evaluate performance across three datasets: a mixed-domain corpora (Data Mix), GSM8K (Cobbe et al., 2021) and the MATH benchmark (Hendrycks et al., 2021).

**Data Mix.** This consists of four distinct domains—*finance*, *creative writing*, *code generation*, and *mathematical reasoning*—sampled respectively from gbharti/finance-alpaca (Bharti, 2023),

Method	Data Mix		GSM8K		MATH	
	LLaMA-3.2	LLaMA-2	LLaMA-3.2	LLaMA-2	LLaMA-3.2	LLaMA-2
Zero-shot prompting (Pretrained)	20.1	33.4	31.3	40.6	12.1	18.8
Finetuning	33.8	48.9	41.5	50.8	23.1	35.4
LoRA Finetuning	33.6	48.1	40.7	47.6	20.4	28.4
Random clustering + LoRA	26.9	38.3	31.2	35.4	15.6	24.3
K-means + LoRA (Mixture of LoRA)	38.8	53.3	44.8	53.1	19.3	32.9
Model Merging	34.1	47.1	30.6	40.7	15.9	27.8
ELREA (Li et al., 2025)	41.7	56.2	43.2	52.4	22.2	41.8
GRADIENTSPACE + SVD init (Ours)	<b>46.4</b>	<b>59.1</b>	<b>46.7</b>	<b>54.7</b>	<b>28.9</b>	<b>46.8</b>

Table 1. Accuracy (%) of different finetuning methods on three benchmarks using **LLaMA-3.2-1B** and **LLaMA-2-7B** models. The best result for each dataset is shown in **bold**, and the second best is underlined.

roneneldan/TinyStories (Eldan & Li, 2023), iamtarun/code\_instructions\_120k\_alpaca (Tarun, 2023), n1ile/hendrycks-MATH-benchmark (Hendrycks et al., 2021). We sample 3,000 examples from each domain to maintain balance and diversity across instruction styles.

Table 1. For a fair comparison, we consider the following baselines:

- **Zero shot prompting.** The unmodified pretraining, without any finetuning.
- **Finetuning.** A single model obtained by finetuning the model on the entire dataset.
- **LoRA Finetuning.** The same training setup as the previous baseline, but instead of updating all model parameters, we only train LoRA adapters.
- **Random clustering + LoRA.** We randomly partition the corpus into a few clusters. For each random cluster we train a distinct LoRA adapter. At inference time we use our router to select which adapter to apply to a given query.
- **K-means + LoRA (Mixture of LoRA).** We embed each training sample, cluster the samples into 5 clusters using K-means over these input embeddings, train one LoRA adapter per cluster, and again use the router at inference time. We perform this experiment three times and report average accuracy.
- **Model merging.** Independently finetuned LoRA adapters (each trained on a disjoint subset of the data) are merged into a single model by linearly combining their weights.
- **ELREA. (Li et al., 2025)** This method partitions the dataset by clustering gradient representations that are compressed to  $d=8192$  using random projection. At inference time, we follow their optimal setting by routing inputs to the full ensemble of experts, aggregating

their predictions via a weighted average derived from softmax-normalized gradient alignment scores.

- **GRADIENTSPACE (Ours).** Our method, in which clusters are defined using gradient similarity. We form clusters by grouping samples whose gradients point in similar update directions, and then train one LoRA adapter per gradient-aligned cluster. Each cluster is partitioned based on our online SVD-based clustering algorithm utilizing full gradient dimension. At inference time, we have a tiny encoder-based classifier to choose the most appropriate expert.

**Results.** Table 1 summarizes results across three benchmarks—Data Mix, GSM8K, and MATH using both LLaMA-3.2-1B and LLaMA-2-7B models. We observe that creating multiple experts with random clustering is ineffective since the accuracy is only 38.3 in DataMix and 24.3 in MATH for example. Next, clustering by input embeddings offers a stronger baseline (i.e.) K-means + LoRA reaches 53.3 on Data Mix and 32.9 on MATH which suggests that routing to specialized adapters helps, though input similarity alone fails to capture how the model actually learns. Furthermore, we explicitly compare our method to ELREA (Li et al., 2025), which employs a weighted ensemble of experts. We find that GRADIENTSPACE outperforms ELREA by an average of 4.2% across all benchmarks, with the most significant gains observed in the MATH domain where our method achieves 22.2% compared to ELREA’s 28.9% (on LLaMA-2). This indicates that ELREA’s strategy of random projection to lower dimension introduces information loss, whereas our approach of strictly routing to a single, SVD-initialized expert effectively isolates conflicting gradients and maximizes specialization. In contrast, GRADIENTSPACE consistently achieves the highest accuracy across all tasks.

**Takeaways.** First, we observe that grouping examples by gradient alignment produces better specialization than grouping by input embeddings, supporting the claim that input similarity is not the same as learning similarity. Next, we

also observe that SVD initialization plays a crucial role in GRADIENTSPACE in identifying gradient conflicts; incorporating SVD-based gradient initialization provides consistent accuracy gains over ELREA (Li et al., 2025). This proves that gradient-based data clustering is a promising direction for scalable instruction tuning.

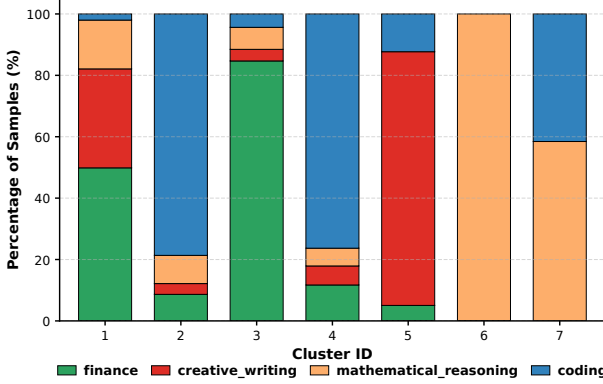


Figure 5. Cluster distribution for Data Mix.

### 6.3 Clustering Analysis

In this section we analyze the effect of applying the GRADIENTSPACE framework to DataMix dataset. The resulting cluster assignments are shown in Figure 5.

**Results** Figure 5 shows that the discovered clusters are not strictly homogeneous by source domain. Even though the data are labeled into clear domains (finance, creative writing, mathematical reasoning, and coding), GRADIENTSPACE groups samples across these domains when their gradients are aligned, i.e., when they reinforce similar model updates. To illustrate the structure of these clusters, we compute TF-IDF statistics within each cluster and list high-weight terms in Table 2.

Cluster	Top Terms
Cluster 1	explain, because, however, example, what, how
Cluster 2	function, list, return, if, price, number, calculate
Cluster 3	stock, market, tax, investment, loan, company, risk, shares, price
Cluster 4	def, return, int, string, for, list, array, len, self, import
Cluster 5	said, happy, little, girl, mom, day, once, time, Lily, Tom
Cluster 6	frac, sqrt, equation, angle, number, sum, proof, \cdot, \align
Cluster 7	prime, number, matrix, array, loop, if/else, calculate

Table 2. High-weight TF-IDF terms per cluster.

These terms indicate that clusters are organized around functional roles rather than strictly around dataset labels. For

example, Cluster 2 mixes procedural language (“function,” “return,” “if”) with numerical/computational terms (“price,” “number,” “calculate”), which spans both coding and finance. Cluster 6 and Cluster 7 both show mathematical structure, but with different emphases: Cluster 6 is associated with formal mathematical presentation (symbols such as  $\cdot$  and LaTeX-style tokens), whereas Cluster 7 emphasizes algorithmic reasoning over mathematical objects (“matrix,” “array,” “loop,” “if/else,” “calculate”), which bridges math reasoning and code.

**Takeaways.** GRADIENTSPACE discovers cross-domain clusters when they yield compatible training signals rather than naive human-provided labels, indicating that gradient alignment captures learning similarity rather than dataset labels. The presence of mixed clusters (e.g., finance with code, math with programmatic reasoning) shows that some instruction types reinforce each other across sources.

### 6.4 Router Performance

We evaluate four router variants to study the trade-off between computational cost and accuracy:

- **Keyword Similarity (KS):** a heuristic router that assigns an expert based on keyword overlap between the input prompt and expert-domain metadata.
- **Embedding Similarity (ES):** computes cosine similarity between the SentenceTransformer embedding (Reimers & Gurevych, 2019) (all-MiniLM-L6-v2) of the input and the mean embedding of each expert’s data.
- **Gradient Similarity (GS) :** matches the input prompt to experts using the stored average gradient vectors per cluster, selecting the expert with the maximum cosine alignment. This formulation is identical to the approach of Li et al. (2025).
- **Semantic Predictor (SP) (Ours):** DistilBERT-like backbone+Linear projector router trained on  $(x_i, k_i)$  pairs as described above.

**Results. and Takeaways.** We summarize the performance of different routers in Table 3. The proposed semantic predictor router achieves **99.4% accuracy** with an average latency of **3.9 ms**, outperforming all other methods in achieving the best accuracy-efficiency tradeoff. Gradient similarity routing provides strong alignment but is prohibitively slow ( $\sim 2000$  ms) due to full gradient computation, while keyword-based heuristics are fast but unreliable (78.5% accuracy).

Table 3. Router design comparison in terms of accuracy and latency.

Router Type	Accuracy (%)	Latency (ms)
KS	78.5	0.01
ES	95.1	5.0
GS (Li et al., 2025)	96.4	2089.3
<b>SP (Ours)</b>	<b>99.4</b>	<b>3.9</b>

Table 4. Computational complexity during inference.

Method	Router FLOPs	Total FLOPs
(Li et al., 2025)	$F_{\text{Base}} + 3F_{\text{LoRA}}$	$(1 + k)F_{\text{Base}} + (3 + k)F_{\text{LoRA}}$
GRADIENTSPACE	$F_{\text{SP}}$ where $F_{\text{SP}} \ll F_{\text{LoRA}}$	$\approx F_{\text{Base}} + F_{\text{LoRA}}$

## 6.5 Computational Complexity

We now compare the computational complexity of ELREA (Li et al., 2025) and our work during inference shown in Table 4. Let us assume the number of floating point operations for one forward pass through a single LoRA adapter is  $F_{\text{LoRA}}$ , for the base model is  $F_{\text{Base}}$  and for our semantic predictor is  $F_{\text{SP}}$ . ELREA relies on per input gradient computation to route among experts, requiring one forward and one backward pass through the LoRA parameters, followed by  $k$  forward passes when ensembling the top- $k$  experts. We assume that approximately backward pass takes twice the flops of forward pass. This results in a total of  $(1 + k)F_{\text{Base}} + (3 + k)F_{\text{LoRA}}$  FLOPs per query. In contrast, GRADIENTSPACE uses gradients only offline to form clusters and train experts, and employs a lightweight semantic router that adds negligible overhead on top of a single expert forward, leading to approximately  $F_{\text{Base}} + F_{\text{LoRA}}$  FLOPs per query.

## 6.6 Ablation: Varying number of clusters

**Experiment** We conduct an ablation study using the MATH dataset by varying the number of clusters  $K$ . To analyze the effect of the number of discovered clusters on cluster quality and final accuracy.

**Results and Takeaways** We show the results of this experiment in Figure 6. We observe that the cluster quality and model accuracy improve as  $K$  increases up to  $K=5$ , beyond which both measures begin to plateau or slightly degrade. This indicates that excessively fine partitioning leads to redundant or noisy gradient clusters that harm generalization, while too few clusters underrepresent the latent structure in the data. To achieve the best trade-off between gradient alignment and downstream performance, we obtain the optimal number of clusters using the validation as described in Section 5.

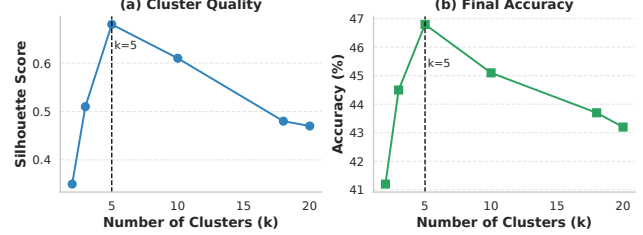


Figure 6. cluster cohesion and Downstream performance varying number of clusters

## 7 CONCLUSION

We introduced GRADIENTSPACE, a framework that clusters instruction tuning data directly in gradient space to mitigate interference. By leveraging online SVD-driven clustering algorithm that allows for utilizing full gradient dimensions, GRADIENTSPACE identifies gradient-aligned groups and finetunes dedicated experts with a lightweight router for inference. Experiments show that it improves accuracy and efficiency over start-of-the-art clustering methods. This demonstrates that organizing data based on gradient dynamics offers a principled path toward scalable, conflict-aware fine-tuning of large language models.

## REFERENCES

Bharti, G. Finance alpaca instruction dataset. <https://huggingface.co/datasets/gbharti/finance-alpaca>, 2023. Hugging Face dataset.

Bukharin, A., Li, S., Wang, Z., Yang, J., Yin, B., Li, X., Zhang, C., Zhao, T., and Jiang, H. Data diversity matters for robust instruction tuning. In Al-Onaizan, Y., Bansal, M., and Chen, Y.-N. (eds.), *Findings of the Association for Computational Linguistics: EMNLP 2024*, pp. 3411–3425, Miami, Florida, USA, November 2024. Association for Computational Linguistics. doi: 10.18653/v1/2024.findings-emnlp.195. URL <https://aclanthology.org/2024.findings-emnlp.195/>.

Chen, S., Jie, Z., and Ma, L. Llava-mole: Sparse mixture of lora experts for mitigating data conflicts in instruction finetuning mllms, 2024. URL <https://arxiv.org/abs/2401.16160>.

Cobbe, K., Kosaraju, V., Bavarian, M., Chen, M., Jun, H., Kaiser, L., Plappert, M., Tworek, J., Hilton, J., Nakano, R., Hesse, C., and Schulman, J. Training verifiers to solve math word problems, 2021. URL <https://arxiv.org/abs/2110.14168>.

DeepSeek-AI et al. Deepseek-r1: Incentivizing reasoning

capability in llms via reinforcement learning, 2025. URL <https://arxiv.org/abs/2501.12948>.

Eldan, R. and Li, Y. Tinystories dataset. <https://huggingface.co/datasets/roneneldan/TinyStories>, 2023. Hugging Face dataset.

et al., H. T. Llama 2: Open foundation and fine-tuned chat models, 2023. URL <https://arxiv.org/abs/2307.09288>.

Ge, Y., Liu, Y., Hu, C., Meng, W., Tao, S., Zhao, X., Xia, M., Li, Z., Chen, B., Yang, H., Li, B., Xiao, T., and Zhu, J. Clustering and ranking: Diversity-preserved instruction selection through expert-aligned quality estimation. In Al-Onaizan, Y., Bansal, M., and Chen, Y.-N. (eds.), *Proceedings of the 2024 Conference on Empirical Methods in Natural Language Processing*, pp. 464–478, Miami, Florida, USA, November 2024. Association for Computational Linguistics. doi: 10.18653/v1/2024.emnlp-main.28. URL <https://aclanthology.org/2024.emnlp-main.28/>.

Ghadimi, S. and Lan, G. Stochastic first-and zeroth-order methods for nonconvex stochastic programming. *SIAM journal on optimization*, 23(4):2341–2368, 2013.

Ghosh, S., Evuru, C. K. R., Kumar, S., S, R., Aneja, D., Jin, Z., Duraiswami, R., and Manocha, D. A closer look at the limitations of instruction tuning. In *Proceedings of the 41st International Conference on Machine Learning*, ICML’24. JMLR.org, 2024.

Grattafiori, A. et al. The llama 3 herd of models. *arXiv preprint arXiv:2407.21783*, 2024.

Han, X., Yang, J., Wang, T., Bi, Z., Hao, J., and Song, J. Towards alignment-centric paradigm: A survey of instruction tuning in large language models, 2025. URL <https://arxiv.org/abs/2508.17184>.

Hendrycks, D. et al. Hendrycks math benchmark. <https://huggingface.co/datasets/nlile/hendrycks-MATH-benchmark>, 2021. Hugging Face dataset wrapper.

Hu, E. J., yelong shen, Wallis, P., Allen-Zhu, Z., Li, Y., Wang, S., Wang, L., and Chen, W. LoRA: Low-rank adaptation of large language models. In *International Conference on Learning Representations*, 2022. URL <https://openreview.net/forum?id=nZeVKeFYf9>.

Koh, P. W. and Liang, P. Understanding black-box predictions via influence functions. In Precup, D. and Teh, Y. W. (eds.), *Proceedings of the 34th International Conference on Machine Learning*, volume 70 of *Proceedings of Machine Learning Research*, pp. 1885–1894. PMLR, 06–11 Aug 2017. URL <https://proceedings.mlr.press/v70/koh17a.html>.

Kwon, Y., Wu, E., Wu, K., and Zou, J. Datainf: Efficiently estimating data influence in lora-tuned llms and diffusion models. In *ICLR*, 2024. URL <https://openreview.net/forum?id=9m02ib92Wz>.

Langley, P. Crafting papers on machine learning. In Langley, P. (ed.), *Proceedings of the 17th International Conference on Machine Learning (ICML 2000)*, pp. 1207–1216, Stanford, CA, 2000. Morgan Kaufmann.

Li, D., Ma, Y., Wang, N., Ye, Z., Cheng, Z., Tang, Y., Zhang, Y., Duan, L., Zuo, J., Yang, C., and Tang, M. Mixlora: Enhancing large language models fine-tuning with lora-based mixture of experts, 2024. URL <https://arxiv.org/abs/2404.15159>.

Li, Y., Gao, V., Zhang, C., and Torkamani, M. Ensembles of low-rank expert adapters. In Yue, Y., Garg, A., Peng, N., Sha, F., and Yu, R. (eds.), *International Conference on Representation Learning*, volume 2025, pp. 92940–92968, 2025. URL [https://proceedings iclr.cc/paper\\_files/paper/2025/file/e8711daef520be07cb9852390c673de8-Paper-Conference.pdf](https://proceedings iclr.cc/paper_files/paper/2025/file/e8711daef520be07cb9852390c673de8-Paper-Conference.pdf).

Liu, B., Liu, X., Jin, X., Stone, P., and Liu, Q. Conflict-averse gradient descent for multi-task learning, 2024. URL <https://arxiv.org/abs/2110.14048>.

Mu, B., Wei, K., Shao, Q., Xu, Y., and Xie, L. Hdmole: Mixture of lora experts with hierarchical routing and dynamic thresholds for fine-tuning llm-based asr models, 2025. URL <https://arxiv.org/abs/2409.19878>.

Muennighoff, N., Tazi, N., Magne, L., and Reimers, N. MTEB: Massive text embedding benchmark. In Vlachos, A. and Augenstein, I. (eds.), *Proceedings of the 17th Conference of the European Chapter of the Association for Computational Linguistics*, pp. 2014–2037, Dubrovnik, Croatia, May 2023. Association for Computational Linguistics. doi: 10.18653/v1/2023.eacl-main.148. URL <https://aclanthology.org/2023.eacl-main.148/>.

Nagaraj, M., Ravikumar, D., and Roy, K. Coresets from trajectories: Selecting data via correlation of loss differences, 2025. URL <https://arxiv.org/abs/2508.20230>.

OpenAI et al. Gpt-4 technical report, 2024. URL <https://arxiv.org/abs/2303.08774>.

Rao, J., Liu, X., Lian, L., Cheng, S., Liao, Y., and Zhang, M. CommonIT: Commonality-aware instruction tuning for large language models via data partitions. In Al-Onaizan, Y., Bansal, M., and Chen, Y.-N. (eds.), *Proceedings of the 2024 Conference on Empirical Methods in*

*Natural Language Processing*, pp. 10064–10083, Miami, Florida, USA, November 2024. Association for Computational Linguistics. doi: 10.18653/v1/2024.emnlp-main.561. URL <https://aclanthology.org/2024.emnlp-main.561/>.

Reimers, N. and Gurevych, I. Sentence-bert: Sentence embeddings using siamese bert-networks. In *Proceedings of the 2019 Conference on Empirical Methods in Natural Language Processing*. Association for Computational Linguistics, 11 2019. URL <https://arxiv.org/abs/1908.10084>.

Schafhalter, P., shun liao, Zhou, Y., Yeh, C.-K., Kandoor, A., and Laudon, J. Scalable multi-domain adaptation of language models using modular experts, 2024. URL <https://openreview.net/forum?id=VAqRZIuW8m>.

Shi, G., Li, Q., Zhang, W., Chen, J., and Wu, X.-M. Recon: Reducing conflicting gradients from the root for multi-task learning, 2023. URL <https://arxiv.org/abs/2302.11289>.

Tarun. Code instructions 120k (alpaca format). [https://huggingface.co/datasets/iamtarun/code\\_instructions\\_120k\\_alpaca](https://huggingface.co/datasets/iamtarun/code_instructions_120k_alpaca), 2023. Hugging Face dataset.

Wang, Z., Zhu, Q., Mi, F., Xu, M., Jin, R., and Yang, W. Clusterucb: Efficient gradient-based data selection for targeted fine-tuning of llms. *ArXiv*, abs/2506.10288, 2025. URL <https://api.semanticscholar.org/CorpusID:279318515>.

Wu, M., Vu, T.-T., Qu, L., and Haf, R. Mixture-of-skills: Learning to optimize data usage for fine-tuning large language models. In Al-Onaizan, Y., Bansal, M., and Chen, Y.-N. (eds.), *Proceedings of the 2024 Conference on Empirical Methods in Natural Language Processing*, pp. 14226–14240, Miami, Florida, USA, November 2024a. Association for Computational Linguistics. doi: 10.18653/v1/2024.emnlp-main.787. URL <https://aclanthology.org/2024.emnlp-main.787/>.

Wu, X., Huang, S., and Wei, F. Mixture of loRA experts. In *The Twelfth International Conference on Learning Representations*, 2024b. URL <https://openreview.net/forum?id=uWvKBCYh4S>.

Xia, M., Malladi, S., Gururangan, S., Arora, S., and Chen, D. Less: selecting influential data for targeted instruction tuning. In *Proceedings of the 41st International Conference on Machine Learning*, ICML’24. JMLR.org, 2024.

Yang, L., Shen, D., Cai, C., Yang, F., Gao, T., ZHANG, D., and Li, X. Solving token gradient conflict in mixture-of-experts for large vision-language model. In *The Thirteenth International Conference on Learning Representations*, 2025. URL <https://openreview.net/forum?id=VxvnV6s1P0>.

Yu, T., Kumar, S., Gupta, A., Levine, S., Hausman, K., and Finn, C. Gradient surgery for multi-task learning. *arXiv preprint arXiv:2001.06782*, 2020.

Zhang, D., Zhang, K., Chu, S., Wu, L., Li, X., and Wei, S. More: A mixture of low-rank experts for adaptive multi-task learning, 2025a. URL <https://arxiv.org/abs/2505.22694>.

Zhang, J., Qin, Y., Pi, R., Zhang, W., Pan, R., and Zhang, T. TAGCOS: Task-agnostic gradient clustered coresset selection for instruction tuning data. In Chiruzzo, L., Ritter, A., and Wang, L. (eds.), *Findings of the Association for Computational Linguistics: NAACL 2025*, pp. 4671–4686, Albuquerque, New Mexico, April 2025b. Association for Computational Linguistics. doi: 10.18653/v1/2025.findings-naacl.264. URL <https://aclanthology.org/2025.findings-naacl.264/>.

Zhang, S., Dong, L., Li, X., Zhang, S., Sun, X., Wang, S., Li, J., Hu, R., Zhang, T., Wu, F., and Wang, G. Instruction tuning for large language models: A survey, 2025c. URL <https://arxiv.org/abs/2308.10792>.

## APPENDIX

### Proof for Lemma 1

Let  $G_i := \nabla \mathcal{L}_i(\theta)$  and  $\mu_i := \mathbb{E}[G_i]$ . Set  $G := \nabla \mathcal{L}(\theta) = \sum_{i=1}^k \alpha_i G_i$  and  $\mu := \mathbb{E}[G] = \sum_{i=1}^k \alpha_i \mu_i$  by linearity of expectation. Using the conventions

$$\text{Var}(X) := \mathbb{E}[\|X - \mathbb{E}X\|^2], \quad \text{Cov}(X, Y) := \mathbb{E}[\langle X - \mathbb{E}X, Y - \mathbb{E}Y \rangle],$$

we have

$$\text{Var}(G) = \mathbb{E}[\|G - \mu\|^2] = \mathbb{E}\left[\left\|\sum_{i=1}^k \alpha_i (G_i - \mu_i)\right\|^2\right],$$

since  $\sum_i \alpha_i \mu_i = \mu$ . Expanding the squared norm and taking expectation gives

$$\begin{aligned} \text{Var}(G) &= \sum_{i=1}^k \alpha_i^2 \mathbb{E}[\|G_i - \mu_i\|^2] + 2 \sum_{1 \leq i < j \leq k} \alpha_i \alpha_j \mathbb{E}[\langle G_i - \mu_i, G_j - \mu_j \rangle] \\ &= \sum_{i=1}^k \alpha_i^2 \text{Var}(G_i) + 2 \sum_{1 \leq i < j \leq k} \alpha_i \alpha_j \text{Cov}(G_i, G_j). \end{aligned}$$

Finally, note that  $2 \sum_{i < j} (\cdot) = \sum_{i \neq j} (\cdot)$ , yielding

$$\text{Var}(\nabla \mathcal{L}(\theta)) = \sum_{i=1}^k \alpha_i^2 \text{Var}(\nabla \mathcal{L}_i(\theta)) + \sum_{i \neq j} \alpha_i \alpha_j \text{Cov}(\nabla \mathcal{L}_i(\theta), \nabla \mathcal{L}_j(\theta)). \quad Q.E.D$$

### Proof of Theorem 2

Let  $g(x) := \nabla \mathcal{L}(\theta; x) \in \mathbb{R}^d$  be the per-example gradient. For any dataset  $\mathcal{D}$ , define

$$\text{Var}(S) := \mathbb{E}_{x \sim \mathcal{D}}[\|g(x) - \mu_{\mathcal{D}}\|^2], \quad \mu_S := \mathbb{E}_{x \sim S}[g(x)].$$

Let  $\mathcal{D}$  be partitioned by GRADIENTSPACE into  $\{\mathcal{D}_i\}_{i=1}^k$  with mixture weights  $p_i := \Pr(x \in \mathcal{D}_i)$  and means  $\mu_{\mathcal{D}_i} := \mathbb{E}_{x \sim \mathcal{D}_i}[g(x)]$ . By the (vector) law of total variance,

$$\text{Var}(\mathcal{D}) = \sum_{i=1}^k p_i \text{Var}(\mathcal{D}_i) + \sum_{i=1}^k p_i \|\mu_{\mathcal{D}_i} - \mu_{\mathcal{D}}\|^2 \geq \sum_{i=1}^k p_i \text{Var}(\mathcal{D}_i). \quad (*)$$

Hence the *average* within-subset variance is never larger than the full-dataset variance:

$$\sum_{i=1}^k p_i \text{Var}(\mathcal{D}_i) \leq \text{Var}(\mathcal{D}). \quad (10)$$

To obtain a uniform per-subset bound, we use the design of GRADIENTSPACE, which minimizes a monotone within-cluster dispersion objective in gradient space. Two standard constructions suffice:

1. **Minimax ( $k$ -center) partition in gradient space.** If GRADIENTSPACE minimizes the maximum within-subset scatter (e.g., a squared-radius / variance proxy), then the trivial one-cluster baseline attains  $\max_i \text{Var}(\mathcal{D}_i) = \text{Var}(\mathcal{D})$ . Optimality therefore implies

$$\max_i \text{Var}(\mathcal{D}_i) \leq \text{Var}(\mathcal{D}),$$

whence  $\text{Var}(\mathcal{D}_i) \leq \text{Var}(\mathcal{D})$  for all  $i$ .

2. **Recursive refinement with a monotone stop rule.** If GRADIENTSPACE splits a cluster only when the children each achieve no larger within-cluster variance than their parent (“refine while reducing”), then starting from the root  $\mathcal{D}$  with  $\text{Var}(\mathcal{D})$  and recursing ensures every leaf  $\mathcal{D}_i$  satisfies

$$\text{Var}(\mathcal{D}_i) \leq \text{Var}(\text{parent}) \leq \text{Var}(\mathcal{D}).$$

Either construction yields the claimed per-subset inequality

$$\text{Var}(\mathcal{D}_i) \leq \text{Var}(\mathcal{D}) \quad \forall i,$$

while (10) shows the result also holds in expectation without any minimax/recursive assumption and is strict whenever the between-subset means differ ( $\sum_i p_i \|\mu_{\mathcal{D}_i} - \mu_{\mathcal{D}}\|^2 > 0$ ).

**Homogeneous-data corollary.** If the dataset is homogeneous in the sense that all subset means coincide with the global mean,  $\mu_{\mathcal{D}_i} = \mu_{\mathcal{D}}$  for all  $i$ , then the between-subset term in (10) is zero and

$$\text{Var}(\mathcal{D}) = \sum_{i=1}^k p_i \text{Var}(\mathcal{D}_i).$$

In particular, when the partition does not reduce within-cluster dispersion (e.g., i.i.d. splitting), we have  $\text{Var}(\mathcal{D}_i) = \text{Var}(\mathcal{D})$  for all  $i$ . Thus, our method is *theoretically performance-neutral* on homogeneous data, and its benefit appears precisely when the data are *heterogeneous*, where the nonzero between-subset term allows variance reduction through specialization.